

Level statistics of XXZ spin chains under zero magnetic field

Kazue Kudo[†], Tetsuo Deguchi[‡]

[†] Graduate School of Humanities and Sciences, Ochanomizu University, 2-1-1 Ohtsuka, Bunkyo-ku, Tokyo 112-8610, Japan

[‡] Department of Physics, Ochanomizu University, 2-1-1 Ohtsuka, Bunkyo-ku, Tokyo 112-8610, Japan

E-mail: [†] kudo@degway.phys.ocha.ac.jp, [‡] deguchi@phys.ocha.ac.jp

Abstract. Level statistics is discussed for XXZ spin chains under zero magnetic field for some values of the next-nearest-neighbour (NNN) coupling parameter. We show how the level statistics of the finite-size systems depends on the NNN coupling and the XXZ anisotropy, which should reflect competition among quantum chaos, integrability and finite-size effects. Evaluating the level-spacing distribution, the spectral rigidity and the number variance, we confirm the correspondence between non-integrability and Wigner behaviour in the spectrum. In particular, Wigner behaviour appears also in the sector of total $S^z = 0$ where spin reversal symmetry exists. Interestingly, the characteristic behaviour of level statistics does not depend on the spectral range for the XXZ spin chains.

PACS numbers: 75.10.Pq, 75.10.Jm, 05.30.-d

1. Introduction

Statistical properties of energy levels have been studied for various physical systems in terms of the random matrix theory (RMT). In quantum spin systems, the RMT analysis has been often quite useful for investigating whether they are integrable or not. It is based on the following conjecture: If a given Hamiltonian is integrable by the Bethe ansatz, the level-spacing distribution should be described by the Poisson distribution:

$$P_{\text{Poi}}(s) = \exp(-s). \quad (1)$$

If it is nonintegrable, the level-spacing distribution should be given by the Wigner distribution:

$$P_{\text{Wig}}(s) = \frac{\pi s}{2} \exp\left(-\frac{\pi s^2}{4}\right). \quad (2)$$

In fact, the behaviour of level-spacing distributions has been numerically confirmed for many quantum spin systems such as correlated spin systems [1, 2, 3, 4, 5, 6, 7] and disordered spin systems [8, 9, 10, 11, 12]. In the Anderson model of disordered systems, $P_{\text{Poi}}(s)$ and $P_{\text{Wig}}(s)$ characterize the localized and the metallic phases, respectively [13].

It should be important to study statistical properties of energy levels for XXZ spin chains, which are related to various important quantum spin chains as well as classical lattice models in two dimensions. Let us consider a spin- $\frac{1}{2}$ XXZ spin chain on L sites with next-nearest-neighbour (NNN) interaction

$$\mathcal{H} = J_1 \sum_{j=1}^L (S_j^x S_{j+1}^x + S_j^y S_{j+1}^y + \Delta_1 S_j^z S_{j+1}^z) + J_2 \sum_{j=1}^L (S_j^x S_{j+2}^x + S_j^y S_{j+2}^y + \Delta_2 S_j^z S_{j+2}^z), \quad (3)$$

where $S^\alpha = (1/2)\sigma^\alpha$ and $(\sigma^x, \sigma^y, \sigma^z)$ are the Pauli matrices; the periodic boundary conditions are imposed. The Hamiltonian (3) is nonintegrable when the NNN coupling J_2 is nonzero, while it is integrable when J_2 vanishes. Here we also note that it coincides with the NNN coupled Heisenberg chain when $\Delta_1 = \Delta_2 = 1$. When J_2 vanishes the system becomes the integrable XXZ spin chain, which is one of the most important integrable quantum spin chains. Here, quantum integrability should lead to Poisson behaviour as the characteristic behaviour of level statistics. When J_2 is nonzero, the characteristic behaviour of level statistics should be given by Wigner behaviour. Here we note that the NNN interaction gives rise to frustration among nearest neighbouring and next-nearest neighbouring spins, which should lead to some chaotic behaviour in the spectrum [14]. In a previous research, however, unexpected behaviour of level-spacing distributions has been found for NNN coupled XXZ spin chains [6]. Robust non-Wigner behaviour has been seen, although the NNN coupled chains are nonintegrable. The non-Wigner behaviour of level-spacing distributions appears particularly when total S^z (S_{tot}^z) = 0, and is roughly given by the average of $P_{\text{Poi}}(s)$ and $P_{\text{Wig}}(s)$. Similar non-Wigner behaviour has been observed for a circular billiard when the angular momentum $L_z = 0$, and for an interacting two-electron system with the Coulomb interaction in a quantum billiard when $L_z = 0$ [15]. Here we should note that Wigner behaviour has been discussed in reference [7] for some XXZ spin chains in sectors of $S_{\text{tot}}^z \neq 0$.

In this paper we show explicitly how the characteristic property of level statistics of the XXZ spin chains should depend on the NNN coupling and the XXZ anisotropy. Here we remark that it should also depend on the system size. Numerically we discuss that the characteristic behaviour of level statistics is determined through competition among quantum chaos, integrability and finite-size effects. Evaluating the level-spacing distribution, the spectral rigidity and the number variance, we confirm the correspondence between non-integrability and Wigner behaviour in the spectrum. In particular, we show that Wigner behaviour appears in a sector of $S_{\text{tot}}^z = 0$, where spin reversal symmetry exists. The spin reversal symmetry has never been taken into account explicitly in previous researches of level statistics partially due to some technical difficulty. However, we have solved the unexpected non-Wigner behaviour. In fact, we explicitly consider two aspects such as mixed symmetry and some finite-size effects appearing near the integrable point. It seems to be rare that such non-Wigner behaviour has been completely understood.

There is another motivation for the present research: another unexpected behaviour of level-spacing distribution has been found for the integrable XXZ chain in reference [6]. The level-spacing distribution $P(s)$ has shown a novel peak at $s = 0$ for the anisotropy parameter $\Delta_1 = 0.5$. The appearance of the peak should be consistent with the sl_2 loop algebra symmetry which appears only for special values of Δ_1 . Here we do not consider Δ_2 since $J_2 = 0$. Let us introduce a parameter q through the relation $\Delta_1 = (q + 1/q)/2$. When q is a root of unity, the integrable XXZ Hamiltonian commutes with the sl_2 loop algebra [16]. Here the loop algebra is an infinite-dimensional Lie algebra, and the dimensions of some degenerate eigenspaces increase exponentially with respect to the system size [17, 18]. Thus the degenerate multiplicity of the non-Abelian symmetry can be extremely large. Furthermore, the sl_2 loop algebra is closely related to Onsager's algebra [19] through which the Ising model was originally solved for the first time. The XXZ spin chains are thus closely related to the most important families of integrable systems through the integrable point, while they are also extended into nonintegrable systems quite naturally. We may therefore expect that the RMT analysis of the XXZ spin chains could be important in discussing level statistics for other quantum systems that would have some connection to an integrable system.

The organization of this paper is the following. In section 2, we recall some aspects of numerical procedure for level statistics. In particular, we explain desymmetrization of the XXZ Hamiltonian. We also remark that in the paper we consider only the XY-like region where $|\Delta| \leq 1$. In section 3, we show how competition among quantum chaos, quantum integrability and finite-size effects should appear in the level statistics of the NNN coupled XXZ spin chains. We evaluate level-spacing distributions, spin rigidities, and number variances, and confirm the RMT correspondence between non-integrability and Wigner behaviour in the spectrum. We solve the non-Wigner behaviour reported in reference [6], explicitly considering the spin reversal symmetry and comparing the numerical results for the sectors of $S_{\text{tot}}^z = 0$ and 1. Here, in order to desymmetrize the XXZ Hamiltonian we formulate the spin reversal operation on lattice fermion operators.

In section 4 we discuss level statistics for a special case of the integrable XXZ spin chain where it has the sl_2 loop algebra symmetry. We observe that there remains many spectral degeneracies in the sector of $S_{\text{tot}}^z = 0$ even after desymmetrization with respect to spin reversal symmetry. Finally, we give conclusions in section 5.

2. Numerical Procedure

Let us discuss desymmetrization of the Hamiltonians of the XXZ spin chains. When performing calculation on level statistics, one has to separate the Hamiltonian matrices into some sectors; in each sector, the eigenstates have the same quantum numbers. The NNN coupled XXZ chains are invariant under spin rotation around the z axis, translation, reflection, and spin reversal. Therefore we consider quantum numbers for the total S^z (S_{tot}^z), the total momentum K_{tot} , the parity, and the spin reversal. However, the parity commutes with the total momentum K_{tot} only when $K_{\text{tot}} = 0$ or π , and the spin reversal commutes with the total S^z only for $S_{\text{tot}}^z = 0$. Thus parity and spin reversal is considered only when $K_{\text{tot}} = 0$ or π and $S_{\text{tot}}^z = 0$, respectively.

It is convenient to use a momentum-based form for the Hamiltonian when we calculate eigenvalues of the NNN coupled chains. To obtain the form, we perform the Jordan-Wigner and the Fourier transformations on the original spin Hamiltonian. Some details are explained in Appendix A. To calculate the eigenvalues, we use standard numerical methods, which are contained in the LAPACK library.

To find universal statistical properties of the Hamiltonians, one has to deal with unfolded eigenvalues instead of raw eigenvalues. The unfolding method is detailed in references [6, 12].

To analyze spectral properties, in this paper, we calculate three quantities: level-spacing distribution $P(s)$, spectral rigidity $\Delta_3(l)$, and number variance $\Sigma^2(l)$. The level-spacing distribution is the probability function $P(s)$ of nearest-neighbor level-spacing $s = x_{i+1} - x_i$, where x_i 's are unfolded eigenvalues. The level-spacing distribution is calculated over the whole spectrum of unfolded eigenvalues unless we specify the range. The spectral rigidity is given by

$$\Delta_3(l) = \left\langle \frac{1}{l} \min_{a,b} \int_{\varepsilon_0-l/2}^{\varepsilon_0+l/2} [N_u(\varepsilon) - a\varepsilon - b]^2 d\varepsilon \right\rangle_{\varepsilon_0}, \quad (4)$$

where $N_u(\varepsilon) = \sum_i \theta(\varepsilon - \varepsilon_i)$ is the integrated density of unfolded eigenvalues and $\langle \rangle_{\varepsilon_0}$ denotes an average over ε_0 . The average is done on the whole spectrum except about 15 levels on each side. The expression of $\Delta_3(l)$ gives the least square deviation of $N_u(\varepsilon)$ from the best fit straight line in an interval l . The number variance is given by

$$\Sigma^2(l) = \left\langle \left[N_u \left(\varepsilon_0 + \frac{l}{2} \right) - N_u \left(\varepsilon_0 - \frac{l}{2} \right) - l \right]^2 \right\rangle_{\varepsilon_0}, \quad (5)$$

where $\langle \rangle_{\varepsilon_0}$ denotes an average over ε_0 . [20] The average is done on the whole spectrum except about 10 levels on each side.

We calculate the spectrum for the 18-site chains with NNN couplings. The matrix size is given by the following: 1387×1387 for $S_{\text{tot}}^z = 0$ and $K_{\text{tot}} = 0$ (Here we do not consider the spin reversal); 1364×1364 for $S_{\text{tot}}^z = 0$ and $K_{\text{tot}} = 2\pi/L$, where L is the number of sites (Here we consider the spin reversal); 1282×1282 for $S_{\text{tot}}^z = 1$ and $K_{\text{tot}} = 0$.

Numerical calculations are performed for the XY-like region, $|\Delta| < 1$, where Δ is the anisotropic parameter. It may be interesting to study for the Ising-like region, $|\Delta| > 1$, because there exist Ising-like magnets. For example, CsCoBr₃ and CsCoCl₃ are quasi-1D Ising-like antiferromagnets with $\Delta \sim 10$ [21]. For $\Delta \gg 1$, however, level statistics is not reliable because energy spectra have some large gaps relative to Δ and the above unfolding method is invalid.

3. Next-Nearest-Neighbor Coupled XXZ Spin Chains

We now discuss numerically in the section that for the XXZ spin chains the characteristic behaviour of level statistics should be determined through competition among quantum chaos, quantum integrability and finite-size effects.

3.1. Spin reversal symmetry and Wigner behaviour for $S_{\text{tot}}^z = 0$

For a sector of $S_{\text{tot}}^z = 0$ we numerically discuss the characteristic behaviour of level statistics on the XXZ spin chains. Here we note that spin reversal symmetry has not been considered explicitly in previous studies of level statistics for various quantum spin chains. In some sense, desymmetrizing the Hamiltonian with respect to spin reversal symmetry has been avoided due to some technical difficulty. Level statistics has been discussed only for sectors of $S_{\text{tot}}^z \neq 0$, where it is not necessary to consider spin reversal symmetry.

Let us show explicitly such a case that Wigner behaviour appears for $S_{\text{tot}}^z = 0$ if we consider spin reversal symmetry. In figure 1 we have obtained the numerical results for level statistics such as the level-spacing distribution $P(s)$, the spectral rigidity $\Delta_3(l)$ and the number variance $\Sigma^2(l)$, for the sector of $K_{\text{tot}} = 2\pi/L$ and $S_{\text{tot}}^z = 0$. Here we note that in the sector the parity invariance does not exist and we can focus on spin reversal symmetry. The numerical results of level statistics shown in figure 1 clearly suggest Wigner behaviour. The curve of the Wigner distribution fits well to the data of the level-spacing distribution $P(s)$. The plots of the spectral rigidity $\Delta_3(l)$ are consistent with the curve of Wigner behaviour as shown in figure 1. It is also the case with the number variance $\Sigma^2(l)$. We have thus confirmed that Wigner behaviour appears also in the sector of $S_{\text{tot}}^z = 0$ for the XXZ spin chains with the NNN interaction.

We now discuss some details of the spin reversal operation. The spin reversal operation on the spin variable of the j th site is defined by

$$S_j^\pm \rightarrow S_j^\mp, \quad S_j^z \rightarrow -S_j^z. \quad (6)$$

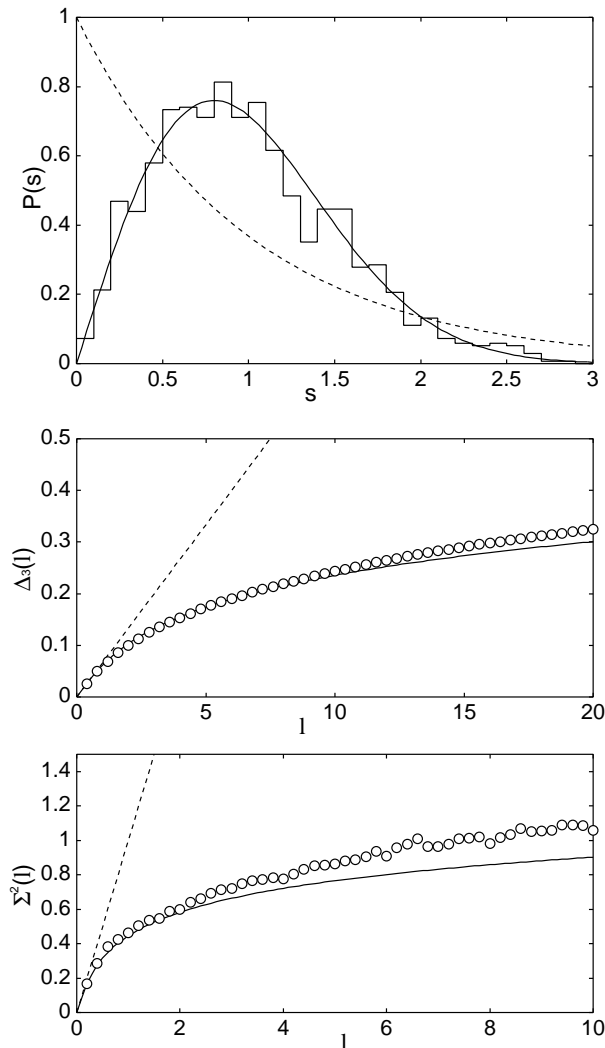


Figure 1. Level-spacing distribution $P(s)$, spectral rigidity $\Delta_3(l)$, and number variance $\Sigma^2(l)$ of the NNN coupled chain for $L = 18$, $J_2/J_1 = 0.5$, $\Delta_1 = \Delta_2 = 0.5$, $S_{\text{tot}}^z = 0$, $K_{\text{tot}} = 2\pi/L$ under consideration of the spin reversal. Broken lines correspond to Poisson behaviour, and solid curves Wigner behaviour.

Here, $S_j^\pm = (S_j^x \pm iS_j^y)/2$. Let M denote the number of down-spins in a given sector. The value of the total spin operator S_{tot}^z is given by $S_{\text{tot}}^z = L/2 - M$. We can show that in a sector of $S_{\text{tot}}^z = L/2 - M$, the transformation of equation (6) corresponds to the following operation on momentum-based fermion operators:

$$\hat{c}_k^\dagger \rightarrow -\hat{c}_{\pi-k}, \quad \hat{c}_k \rightarrow -\hat{c}_{\pi-k}^\dagger. \quad (7)$$

Here, \hat{c}_k^\dagger and \hat{c}_k are the creation and annihilation operators of free fermions with momentum k . In Appendix A we discuss the definition of the fermion operators through the Jordan-Wigner transformation. We note that the value of momentum k is given by $(2\pi/L) \times (\text{an integer})$ for odd M and $(2\pi/L) \times (\text{a half-integer})$ for even M . An explicit derivation of the transformation (7) from the definition (6) is given in Appendix B.

When desymmetrizing the Hamiltonian with respect to spin reversal symmetry, it is useful to know how the vacuum state transforms under the spin reversal operation expressed in terms of the momentum-based fermion operators. Let us denote by $|0\rangle$ the vacuum state where there is no down-spin. Under the spin reversal operation it transforms upto a phase factor A_L as follows

$$|0\rangle \rightarrow A_L \hat{c}_{q_1}^\dagger \hat{c}_{q_2}^\dagger \cdots \hat{c}_{q_L}^\dagger |0\rangle \quad (8)$$

Here q_j denotes momentum $(2\pi/L)j$ for $j = 1, 2, \dots, L$, when M is odd, and $(2\pi/L)(j - 1/2)$ for $j = 1, 2, \dots, L$, when M is even. We can show that the phase factor A_L is given by

$$A_L = \frac{1}{L^{L/2}} \sum_{P \in \mathcal{S}_L} \epsilon_P \exp(-i \sum_{j=1}^L j k_{Pj}). \quad (9)$$

Here \mathcal{S}_L denotes the set of permutations on L elements, ϵ_P the sign of permutation P . Furthermore, we can calculate the phase factor A_L as follows

$$A_L = \begin{cases} (-1)^\ell & \text{for } M = 2\ell \\ (-1)^{\ell+1} & \text{for } M = 2\ell + 1 \end{cases} \quad (10)$$

The derivation is given in Appendix C.

It is sometimes convenient to use the following in stead of equation (7):

$$\hat{c}_k^\dagger \rightarrow \hat{c}_{\pi-k}, \quad \hat{c}_k \rightarrow \hat{c}_{\pi-k}^\dagger. \quad (11)$$

The Hamiltonians are invariant not only for equation (7) but also for equation (11). The form (11) has an advantage that we do not need to consider the phase factor -1 that appears in equation (7).

Making use of the spin reversal operation expressed in terms of the fermion basis (11) we have desymmetrized the Hamiltonian matrix in the sector $S_{\text{tot}}^z = 0$ with respect to spin reversal symmetry. For a given vector with $S_{\text{tot}}^z = 0$ we calculate how it transforms under the operation (11). If it is not a singlet and transforms into a different vector, then we combine the pair into an eigenvector of the operation (11). We have thus obtained the Wigner behaviour of the level statistics as shown in figure 1.

3.2. Finite-size effects on the level spacing distribution

Let us explicitly discuss finite-size effects appearing in level statistics. They should be important in the Poisson-like or non-Wigner behaviour observed in level statistics for the completely desymmetrized XXZ Hamiltonians. There are two regions in which finite-size effects are prominent: A region where J_2 is close to zero and another region where Δ_1 and Δ_2 are close to 1. In the former region quantum integrability appears through finite-size effects, and the characteristic behaviour of level statistics becomes close to Poisson-like behaviour. In the latter region, Poisson-like behaviour appears due to the symmetry enhancement at the point of $\Delta_1 = \Delta_2 = 1$, where the $U(1)$ symmetry of the XXZ spin chain expands into the spin $SU(2)$ symmetry.

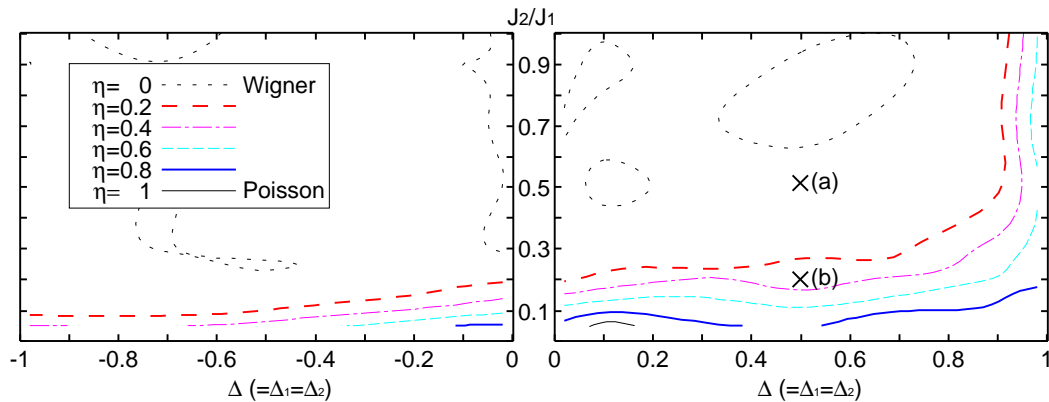


Figure 2. The diagram of contour lines of η for the NNN coupled chain with $L = 18$, in the sector of $S_{\text{tot}}^z = 1$ and $K_{\text{tot}} = 0$. Roughly speaking, the area above the long red dashed line, Wigner behaviour; the area below the blue solid line, Poisson behaviour. The points (a) and (b) correspond to figures 3(a) and 3(b), respectively.

Let us now discuss how the degree of non-Wigner behaviour depends on the anisotropy parameters, Δ_1 and Δ_2 , and the NNN coupling, J_2 . For simplicity we set $\Delta_1 = \Delta_2$ and denote it by Δ , and we also consider the ratio of J_2/J_1 . We express the degree of non-Wigner behaviour by the following parameter:

$$\eta = \frac{\int_0^{s_0} [P(s) - P_{\text{Wig}}(s)] ds}{\int_0^{s_0} [P_{\text{Poi}}(s) - P_{\text{Wig}}(s)] ds}, \quad (12)$$

where $s_0 = 0.4729 \dots$ is the intersection point of $P_{\text{Poi}}(s)$ and $P_{\text{Wig}}(s)$ [9, 12]. We have $\eta = 0$ when $P(s)$ coincides with $P_{\text{Wig}}(s)$, and $\eta = 1$ when $P(s)$ coincides with $P_{\text{Poi}}(s)$. The diagram of contour lines of η is shown in figure 2. We have calculated them for the area $-0.98 \leq \Delta \leq -0.02$, $0.02 \leq \Delta \leq 0.98$, and $0.02 \leq J_2/J_1 \leq 1$, where $\Delta = \Delta_1 = \Delta_2$.

The contour lines of η show that a behaviour close to Wigner one appears in a large region, while the Poisson-like behaviour appears in a narrow region along the line of $J_2/J_1 = 0$ and that of $\Delta_1 = \Delta_2 = 1$. The Poisson-like behaviour is dominated by finite-size effects and hence should vanish when $L \rightarrow \infty$. This expectation should be consistent with the suggestion in reference [7] that an infinitesimal integrability-breaking term (the NNN term of equation (3) in this paper) would lead to Wigner behaviour. Here we remark that the phase diagrams of the ground state [22, 23] are totally different from the diagram of contour lines of η . It is due to the fact that level statistics reflects highly excited states rather than the ground state.

When $\Delta_1 = \Delta_2 = 0.98$, Poisson-like behaviour appears in level statistics due to some finite-size effects. It will be explicitly shown in figures 4 and 5. When $\Delta_1 = \Delta_2 = 1$, equation (3) coincides with the Heisenberg chain, which has the spin $SU(2)$ symmetry. Some degenerate energy levels at $\Delta_1 = \Delta_2 = 1$ can become nondegenerate when Δ_1 and Δ_2 are not equal to 1. The difference among the nondegenerate energy levels should be smaller than the typical level spacing when Δ_1 and Δ_2 are close to 1. The typical level spacing, which is of the order of $1/L$, should become large when the system size L

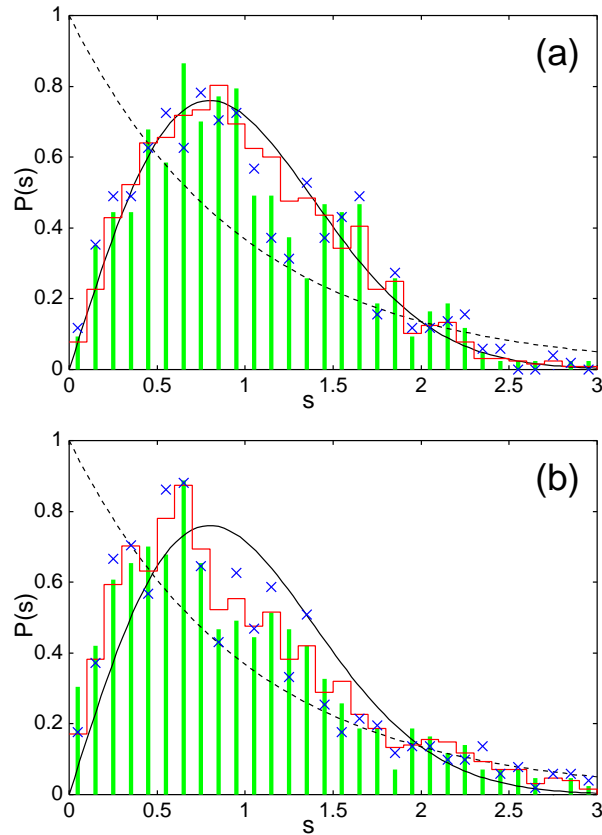


Figure 3. Level-spacing distribution of the NNN coupled chain for $L = 18$, $\Delta_1 = \Delta_2 = 0.5$, $S_{\text{tot}}^z = 1$, and (a) $J_2/J_1 = 0.5$; (b) $J_2/J_1 = 0.2$. Red histograms are for all levels; green bars, 1/3 of all levels around the centre; blue crosses, 10% of all levels from each of the two edges. Solid and broken lines show the Wigner and Poisson distributions, respectively.

is small. Thus, the Poisson-like behaviour should practically appear in level statistics. We note that for the Heisenberg chain Wigner behaviour appears in the level-spacing distribution when we desymmetrize the Hamiltonian with respect to the spin $SU(2)$ symmetry [2, 3].

3.3. Homogeneity of the characteristic behaviour of level statistics throughout the spectrum

Let us discuss that for the XXZ spin chains the characteristic behaviour of level statistics does not depend on the energy range of the spectrum. In figure 3, we show level-spacing distributions evaluated at points (a) and (b) shown in the diagram of figure 2. They are evaluated for three different energy ranges. The distributions shown in figure 3(a) give Wigner behaviour, while the distributions of figure 3(b) are close to Poisson behaviour.

Let us explain the three different energy ranges shown in figure 3. Red histograms show the level-spacing distributions evaluated for all levels, while green bars show those

evaluated only for the 1/3 of all levels around the centre, and blue crosses for the 10% of all levels located from each of the two spectral edges.

Quite interestingly, the distributions evaluated for the different energy ranges are quite similar to each other. Here we should note that some statistical 'noises' exist but they are rather small. This makes a remarkable contrast between the level-spacing distributions of the XXZ spin chains and that of the Anderson model of disordered systems. Here we recall that even in the metallic phase the level-spacing distribution of the Anderson model shows Poisson behaviour if we evaluate it around the two edge regions of the energy spectrum.

3.4. Two solutions to unexpected non-Wigner behaviour: mixed symmetry and finite-size effects

Unexpected non-Wigner behaviour has been reported in reference [6] for level-spacing distributions of the NNN coupled XXZ chains. Let us discuss the reason why it was observed, considering both mixed symmetry and finite-size effects. There are two types of non-Wigner profiles for the nonintegrable systems: one is given by almost the numerical average of the Poisson and the Wigner distributions, and another one is rather close to the Poisson distribution. The profiles of the first type appear in various cases [6], such as the case of $\Delta_2 = 0.5$. The profiles of the second type appear in particular for the case of $\Delta_1 \simeq \Delta_2 \simeq 1$. We may call the latter Poisson-like behaviour rather than simple non-Wigner behaviour. Both types of non-Wigner distributions have been observed in the subspace of $S_{\text{tot}}^z = 0$, which is the largest sector of the Hamiltonian matrix of equation (3). Here we note that the observations in reference [6] for $S_{\text{tot}}^z = 0$ do not contradict with the Wigner behaviour of reference [7] for $S_{\text{tot}}^z \neq 0$, where the level-spacing distributions of similar XXZ chains have been discussed.

We show level-spacing distributions in figure 4 for the four cases: $S_{\text{tot}}^z = 0$ or 1 and $\Delta_1 = \Delta_2 = 0.5$ or 0.98. The numerical results suggest that the value of S_{tot}^z should be important as well as the anisotropy parameters, Δ_1 and Δ_2 , in the observed non-Wigner behaviour of the level-spacing distributions. When $\Delta_1 = \Delta_2 = 0.5$, Wigner behaviour appears for $S_{\text{tot}}^z = 1$, while the non-Wigner behaviour was observed for $S_{\text{tot}}^z = 0$. We have also checked that Wigner behaviour appears for $S_{\text{tot}}^z = 2$. Furthermore, we have confirmed that such S_{tot}^z -dependence of the level-spacing distribution is valid for some values of K_{tot} . Here we have desymmetrized the Hamiltonian according to S_{tot}^z , K_{tot} , and the parity when it exists, but not to the spin reversal. Here we note that the parity invariance exists only for sectors with $K_{\text{tot}} = 0$ or π when L is even.

The non-Wigner behaviour observed for the case $S_{\text{tot}}^z = 0$ and $\Delta_1 = \Delta_2 = 0.5$ shown in figure 4 should be due to mixed symmetry. We have not considered spin reversal symmetry which is important only for $S_{\text{tot}}^z = 0$. Let us recall the Wigner behaviour for $S_{\text{tot}}^z = 0$ shown in figure 1. It is for $K_{\text{tot}} = 2\pi/L$. However, Wigner behaviour should appear also for the sector of $K_{\text{tot}} = 0$ and $S_{\text{tot}}^z = 0$ where we have to consider both the parity and the spin reversal operations simultaneously. The behaviour

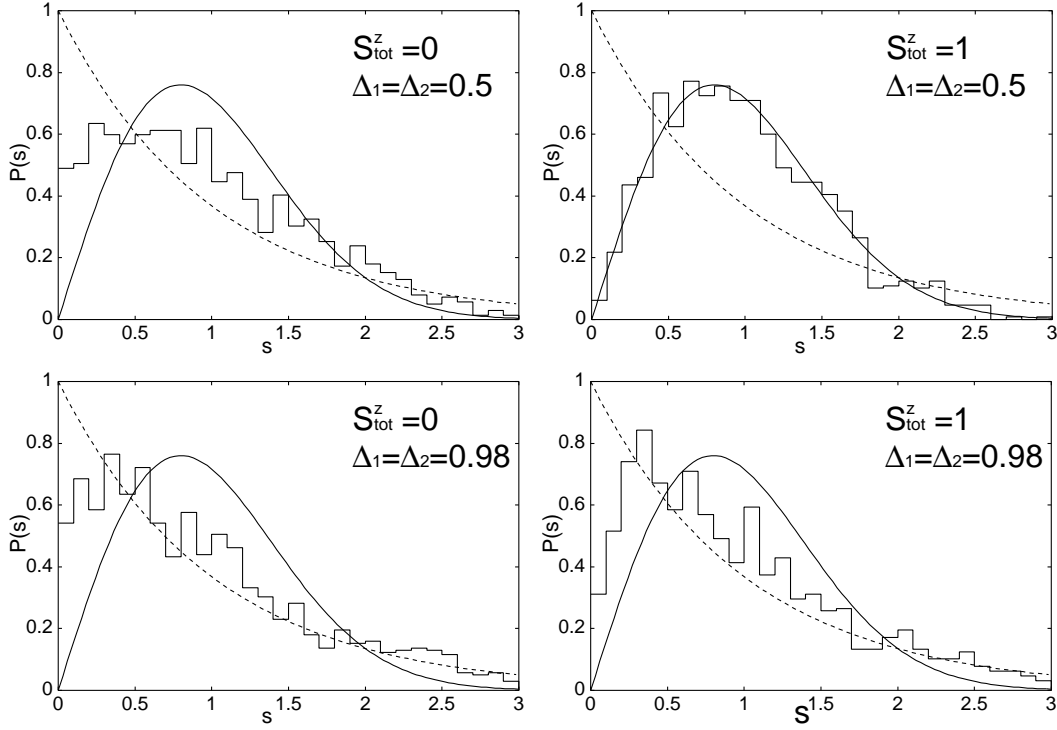


Figure 4. Level-spacing distribution $P(s)$ of the NNN coupled chain for $L = 18$, $J_2/J_1 = 1$, $K_{\text{tot}} = 0$. Broken lines, the Poisson distribution; solid curves, the Wigner distribution.

of level statistics should be independent of K_{tot} .

The Poisson-like behaviour for the case $\Delta_1 = \Delta_2 = 0.98$ should be dominated by finite-size effects. In fact, for $S_{\text{tot}}^z = 1$ of figure 4, the Poisson-like behaviour appears when $\Delta_1 = \Delta_2 = 0.98$, while Wigner behaviour appears when $\Delta_1 = \Delta_2 = 0.5$. We have confirmed that such tendency does not depend on the value of K_{tot} : we see it not only for $K_{\text{tot}} = 0$ but also for $K_{\text{tot}} \neq 0$. We discuss the finite-size effects on this model in section 3.2

The observations of the level-spacing distributions can also be confirmed by investigating spectral rigidity $\Delta_3(l)$ and number variance $\Sigma^2(l)$. In figure 5, $\Delta_3(l)$ and $\Sigma^2(l)$ are shown for the four cases corresponding to those of figure 4. For $S_{\text{tot}}^z = 1$ and $\Delta_1 = \Delta_2 = 0.5$, Wigner behaviour appears. For $S_{\text{tot}}^z = 0$ and $\Delta_1 = \Delta_2 = 0.5$, an intermediate behaviour appears, which is close to the average between Wigner and Poisson behaviours. For $\Delta_1 = \Delta_2 = 0.98$, both for $S_{\text{tot}}^z = 0$ and $S_{\text{tot}}^z = 1$, Poisson-like behaviour appears for $\Delta_3(l)$ and $\Sigma^2(l)$.

It should be possible to show explicitly Wigner behaviour for $S_{\text{tot}}^z = 0$ and $K_{\text{tot}} = 0$. However, it is not technically straightforward. In the sector of $S_{\text{tot}}^z = 0$ and $K_{\text{tot}} = 0$, we have to construct sub-sectors according to the eigenvalues of the parity and the spin reversal operations. In terms of momentum-based fermion operators, the parity

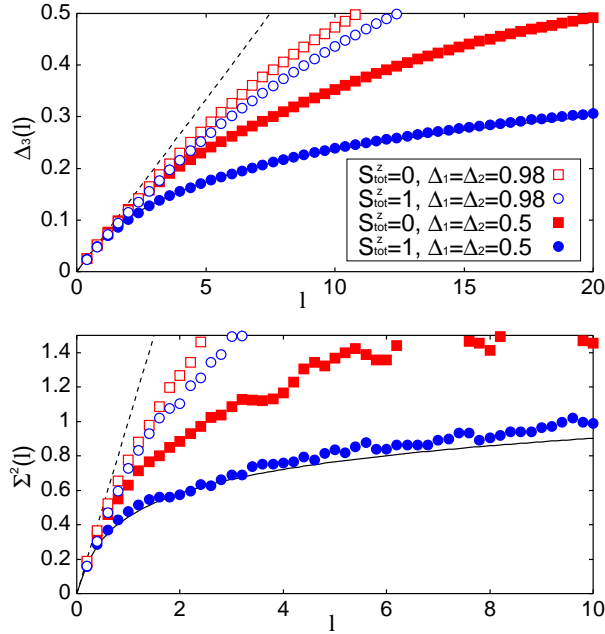


Figure 5. Spectral rigidity $\Delta_3(l)$ and number variance $\Sigma^2(l)$ of the NNN coupled chain for $L = 18$, $J_2/J_1 = 1$, $K_{\text{tot}} = 0$. Broken lines, Poisson behaviour; Solid lines, Wigner behaviour. In each of the four distributions $P(s)$ vanishes at $s = 0$: there is no degeneracy among energy levels.

operation is given by

$$\hat{c}_k^\dagger \rightarrow e^{ik} \hat{c}_{-k}^\dagger (-1)^{M-1+L/2-S_{\text{tot}}^z}, \quad \hat{c}_k \rightarrow e^{-ik} \hat{c}_{-k} (-1)^{M+L/2-S_{\text{tot}}^z} \quad (13)$$

Here we recall that M denotes the number of down-spins in the sector of $S_{\text{tot}}^z = L/2 - M$. Through the Jordan-Wigner transformation we can easily derive the parity operation (13) from that on the spin variables: $\sigma_\ell^\pm \rightarrow \sigma_{L+1-\ell}^\pm$, $\sigma_\ell^z \rightarrow \sigma_{L+1-\ell}^z$ for $\ell = 1, 2, \dots, L$.

4. Integrable XXZ Spin Chain in a special case

Let us discuss level statistics for the special case of the integrable XXZ spin chain that has the sl_2 loop algebra symmetry. Here we recall that the XXZ spin chain is integrable when the NNN coupling J_2 vanishes, and also that the sl_2 loop algebra symmetry exists when q is a root of unity. Here the anisotropy Δ_1 is related to q through $\Delta_1 = (q+q^{-1})/2$. For instance, when the parameter q is given by $\exp(i\pi/3)$, we have $\Delta = 0.5$.

The level spacing distribution $P(s)$ and the spectral rigidity $\Delta_3(\ell)$ of the integrable XXZ spin chain are shown for $\Delta_1 = 0.5$ in figure 6. In figure 6 (a) we do not consider the spin reversal symmetry, while in figure 6 (b) we plot the level-spacing distribution $P(s)$ and the spectral rigidity $\Delta_3(\ell)$ after we desymmetrize the Hamiltonian with respect to the spin reversal operation.

We observe that there still remain many degeneracies associated with the sl_2 loop algebra symmetry, even after desymmetrizing the Hamiltonian with respect to spin

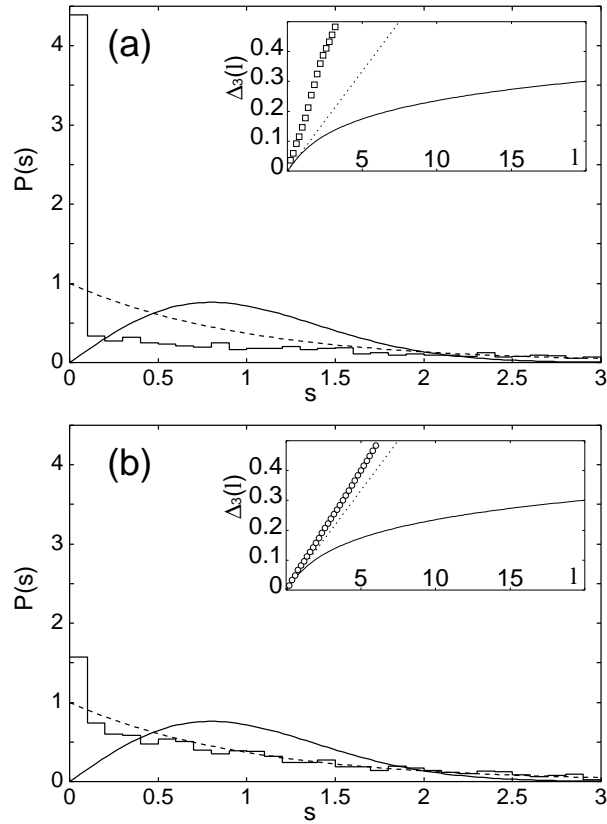


Figure 6. Level-spacing distribution $P(s)$ of the integrable chain ($J_2 = 0$) for $L = 18$, $\Delta_1 = 0.5$, $S_{\text{tot}}^z = 0$, $K_{\text{tot}} = 2\pi/L$, (a) not considering the spin reversal; (b) considering the spin reversal. The inset is spectral rigidity for each case.

reversal symmetry. The level-spacing distribution $P(s)$ has a small peak at $s = 0$ in figure 6 (b). Furthermore, the slopes of $\Delta_3(l)$ shown in the insets of figure 6 (a) and (b) are larger than that of Poisson behaviour. However, the numerical result does not necessarily give a counterexample to the conjecture of RMT. The level statistics might show Poisson behaviour, if we completely desymmetrize the Hamiltonian matrix in terms of the sl_2 loop algebra symmetry.

5. Conclusions

For the finite spin- $\frac{1}{2}$ XXZ spin chains with the NNN interaction, we have evaluated characteristic quantities of level statistics such as the level-spacing distribution, the spectral rigidity and the number variance. Through the numerical results we have obtained the following conjecture: When the symmetry of a finite-size system enhances at some point of the parameter space, the characteristic behaviour of level statistics should be given by Poisson-like behaviour near some region close to the point. In particular, we have shown that finite-size effects play an important role in the characteristic quantities of level statistics for the XXZ spin chains. Here they are

integrable for $J_2 = 0$, and their $U(1)$ symmetry extends into $SU(2)$ symmetry at the point of $\Delta_1 = \Delta_2 = 1$. Furthermore, we have also shown that some unexpected behaviour can appear when an extra symmetry is not taken into account, such as the case of the spin reversal symmetry in the sector of $S_{\text{tot}}^z = 0$. Here we note that extra symmetries may depend on some parameters as well as some quantum numbers. We have thus solved completely the observed non-Wigner behaviours of NNN coupled chain for $S_{\text{tot}}^z = 0$ in reference [6].

Acknowledgments

The authors would like to thank K. Nakamura and T. Kato for useful discussions. The authors also thank the Yukawa Institute for Theoretical Physics at Kyoto University. Discussions during the YITP workshop YITP-W-03-16 on ‘‘Quantum Mechanics and Chaos: From Fundamental Problems through Nanosciences’’ were useful to complete this work. The present study was partially supported by the Grant-in-Aid for Encouragement of Young Scientists (A): No. 14702012. It was also partially supported by Hayashi Memorial Foundation for Female Natural Scientists.

Appendix A. Jordan-Wigner and Fourier Transformations

Let us rewrite equation (3) by

$$\begin{aligned} \mathcal{H} &= \mathcal{H}_1 + \mathcal{H}_2 \\ &= J_1 \sum_{l=1}^L (S_l^x S_{l+1}^x + S_l^y S_{l+1}^y + \Delta_1 S_l^z S_{l+1}^z) + J_2 \sum_{l=1}^L (S_l^x S_{l+2}^x + S_l^y S_{l+2}^y + \Delta_2 S_l^z S_{l+2}^z), \end{aligned} \quad (\text{A.1})$$

where \mathcal{H}_1 is the term containing nearest-neighbor couplings and \mathcal{H}_2 is the term containing next-nearest-neighbor couplings. We define the Jordan-Wigner transformation by

$$\sigma_l^- = \exp\left(-i\pi \sum_{j=1}^{l-1} c_j^\dagger c_j\right) c_l^\dagger, \quad (\text{A.2})$$

$$\sigma_l^+ = \exp\left(i\pi \sum_{j=1}^{l-1} c_j^\dagger c_j\right) c_l, \quad (\text{A.3})$$

$$\sigma_l^z = 2\sigma_l^+ \sigma_l^- - 1 = 1 - 2\sigma_l^- \sigma_l^+, \quad (\text{A.4})$$

where c_j^\dagger and c_j are the creation and annihilation operators of fermions on j th site. Under the Jordan-Wigner transformation, \mathcal{H}_1 is written by

$$\begin{aligned} \mathcal{H}_1 &= \frac{J_1}{4} \Delta_1 \left(L - 2 \sum_{l=1}^L c_l^\dagger c_l \right) \\ &+ \frac{J_1}{4} \sum_{l=1}^{L-1} [2(c_l^\dagger c_{l+1} + c_{l+1}^\dagger c_l) + \Delta_1 (4c_l^\dagger c_l c_{l+1}^\dagger c_{l+1} - 2c_{l+1}^\dagger c_{l+1})] \\ &+ \frac{J_1}{4} [2(c_L^\dagger c_{L+1} + c_{L+1}^\dagger c_L) + \Delta_1 (4c_L^\dagger c_L c_{L+1}^\dagger c_{L+1} - 2c_{L+1}^\dagger c_{L+1})]. \end{aligned} \quad (\text{A.5})$$

Here, we consider periodic boundary conditions ($\sigma_{L+1}^\pm = \sigma_1^\pm$):

$$\begin{aligned} c_{L+1} &= \exp\left(-i\pi \sum_{j=1}^L \sigma_j^- \sigma_j^+\right) \sigma_{L+1}^+ = \exp\left(-\frac{i\pi L}{2} + \frac{i\pi}{2} \sum_{j=1}^L \sigma_j^z\right) \sigma_1^+ \\ &= \sigma_1^+ \exp\left[i\pi \left(-\frac{L}{2} + S_{\text{tot}}^z + 1\right)\right], \\ c_{L+1}^\dagger &= \exp\left(i\pi \sum_{j=1}^L \sigma_j^- \sigma_j^+\right) \sigma_{L+1}^- = \exp\left(\frac{i\pi L}{2} - \frac{i\pi}{2} \sum_{j=1}^L \sigma_j^z\right) \sigma_1^- \\ &= \sigma_1^- \exp\left[i\pi \left(\frac{L}{2} - S_{\text{tot}}^z + 1\right)\right], \end{aligned} \quad (\text{A.6})$$

where we use $e^{S_1^z} \sigma_1^\pm = \sigma_1^\pm e^{S_1^z \pm 1}$. Since $\sigma_1^+ = c_1$, $\sigma_1^- = c_1^\dagger$, and $S_{\text{tot}}^z = (L-M)/2 - M/2 = L/2 - M$, where M is the number of fermions, we have

$$c_{L+1} = -(-1)^M c_1, \quad c_{L+1}^\dagger = -(-1)^M c_1^\dagger. \quad (\text{A.7})$$

Therefore, \mathcal{H}_1 is rewritten by

$$\begin{aligned} \mathcal{H}_1 &= \frac{J_1}{4} \Delta_1 \left[L + \sum_{l=1}^L (4c_l^\dagger c_l c_{l+1}^\dagger c_{l+1} - 4c_l^\dagger c_l) \right] \\ &\quad + \frac{J_1}{4} \cdot 2 \left[\sum_{l=1}^{L-1} (c_l^\dagger c_{l+1} + c_{l+1}^\dagger c_l) - (-1)^M (c_L^\dagger c_1 + c_1^\dagger c_L) \right]. \end{aligned} \quad (\text{A.8})$$

Now, we define the Fourier transformation as

$$c_l = \frac{1}{\sqrt{L}} \sum_k \hat{c}_k e^{ikl}, \quad (\text{A.9})$$

$$c_l^\dagger = \frac{1}{\sqrt{L}} \sum_k \hat{c}_k^\dagger e^{-ikl}. \quad (\text{A.10})$$

Here, k takes $(2\pi/L) \times$ (an integer) for odd M and $(2\pi/L) \times$ (a half-integer) for even M , and $0 \leq k < 2\pi$. After the Fourier transformation,

$$\begin{aligned} \mathcal{H}_1 &= \frac{J_1}{4} \Delta_1 L + J_1 \sum_k (\cos k - \Delta_1) \hat{c}_k^\dagger \hat{c}_k \\ &\quad - \frac{J_1 \Delta_1}{L} \sum_{k_1, k_2, k_3, k_4} \delta_{k_1+k_2, k_3+k_4} \exp[-i(k_2 - k_4)] \hat{c}_{k_1}^\dagger \hat{c}_{k_2}^\dagger \hat{c}_{k_3} \hat{c}_{k_4}, \end{aligned} \quad (\text{A.11})$$

where

$$\delta_{k_1+k_2, k_3+k_4} = \begin{cases} 1 & \text{when } k_1 + k_2 \pmod{L} = k_3 + k_4 \pmod{L}. \\ 0 & \text{otherwise.} \end{cases} \quad (\text{A.12})$$

Considering combination of k 's, we can rewrite equation (A.11) by

$$\begin{aligned} \mathcal{H}_1 &= J_1 \Delta_1 \left(\frac{L}{4} - M \right) + J_1 \sum_k \cos k \hat{c}_k^\dagger \hat{c}_k \\ &\quad - \frac{2J_1 \Delta_1}{L} \sum_{\substack{k_1 < k_2 \\ k_3 > k_4}} \delta_{k_1+k_2, k_3+k_4} [\cos(k_2 - k_4) - \cos(k_2 - k_3)] \hat{c}_{k_1}^\dagger \hat{c}_{k_2}^\dagger \hat{c}_{k_3} \hat{c}_{k_4}. \end{aligned} \quad (\text{A.13})$$

In the same way, \mathcal{H}_2 can be rewritten by

$$\begin{aligned} \mathcal{H}_2 &= J_2 \Delta_2 \left(\frac{L}{4} - M \right) + J_2 \sum_k \cos 2k \hat{c}_k^\dagger \hat{c}_k \\ &+ \frac{2J_2}{L} \sum_{\substack{k_1 < k_2 \\ k_3 > k_4}} \delta_{k_1+k_2, k_3+k_4} [\cos(k_1 + k_3) + \cos(k_2 + k_4) - \cos(k_1 + k_4) - \cos(k_2 + k_3)] \hat{c}_{k_1}^\dagger \hat{c}_{k_2}^\dagger \hat{c}_{k_3} \hat{c}_{k_4} \\ &- \frac{2J_2 \Delta_2}{L} \sum_{\substack{k_1 < k_2 \\ k_3 > k_4}} \delta_{k_1+k_2, k_3+k_4} \{ \cos [2(k_2 - k_4)] - \cos [2(k_2 - k_3)] \} \hat{c}_{k_1}^\dagger \hat{c}_{k_2}^\dagger \hat{c}_{k_3} \hat{c}_{k_4}. \end{aligned} \quad (\text{A.14})$$

Appendix B. Spin reversal symmetry on momentum-based fermions

Let us find the momentum-based expression of the mapping corresponding to the spin reversal transformation ($S_j^\pm \rightarrow S_j^\mp$, $S_j^z \rightarrow -S_j^z$). According to equations (A.2), (A.3), (A.9), and (A.10),

$$\hat{c}_k = \frac{1}{\sqrt{L}} \sum_{l=1}^L \exp(-ikl) \exp \left(-i\pi \sum_{j=1}^{l-1} \sigma_j^- \sigma_j^+ \right) \sigma_l^+, \quad (\text{B.1})$$

$$\hat{c}_k^\dagger = \frac{1}{\sqrt{L}} \sum_{l=1}^L \exp(ikl) \exp \left(i\pi \sum_{j=1}^{l-1} \sigma_j^- \sigma_j^+ \right) \sigma_l^-. \quad (\text{B.2})$$

Under the transformation $\sigma_l^\pm \rightarrow \sigma_l^\mp$, equations (B.1) and (B.2) is transformed as the following.

$$\begin{aligned} \hat{c}_k &\rightarrow \frac{1}{\sqrt{L}} \sum_{l=1}^L \exp(-ikl) \exp \left(-i\pi \sum_{j=1}^{l-1} \sigma_j^+ \sigma_j^- \right) \sigma_l^- \\ &= \frac{1}{\sqrt{L}} \sum_{l=1}^L \exp(-ikl) \exp \left[-i\pi \sum_{j=1}^{l-1} (I_j - \sigma_j^- \sigma_j^+) \right] \sigma_l^- \\ &= \frac{1}{\sqrt{L}} \sum_{l=1}^L \exp[-ikl - i\pi(l-1)] \exp \left(i\pi \sum_{j=1}^{l-1} \sigma_j^- \sigma_j^+ \right) \sigma_l^-, \end{aligned} \quad (\text{B.3})$$

where I_j is the unit matrix. Now, considering $e^{2\pi il} = 1$, where l is an integer, we can find that

$$\begin{aligned} \exp[-ikl - i\pi(l-1)] &= \exp[-ikl - i\pi(l-1) + 2\pi il] = \exp[i(\pi - k)l + i\pi] \\ &= -\exp[i(\pi - k)l]. \end{aligned} \quad (\text{B.4})$$

Therefore, equation (B.3) is rewritten as

$$\hat{c}_k \rightarrow -\frac{1}{\sqrt{L}} \sum_{l=1}^L \exp[i(\pi - k)l] \exp \left(i\pi \sum_{j=1}^{l-1} \sigma_j^- \sigma_j^+ \right) \sigma_l^- = -\hat{c}_{\pi-k}^\dagger. \quad (\text{B.5})$$

In the same way, we can show

$$\hat{c}_k^\dagger \rightarrow -\hat{c}_{\pi-k}. \quad (\text{B.6})$$

Appendix C. Spin reversal operation on the vacuum state

Let us introduce the following matrix:

$$U_s = \prod_{j=1}^L \sigma_j^x. \quad (\text{C.1})$$

We may express the spin reversal operation (6) as follows

$$\begin{aligned} U_s S_j^\pm U_s^{-1} &= S_j^\mp, & U_s S_j^z U_s^{-1} &= -S_j^z \\ U_s \hat{c}_k^\dagger U_s^{-1} &= -\hat{c}_{\pi-k}, & U_s \hat{c}_k U_s^{-1} &= -\hat{c}_{\pi-k}^\dagger. \end{aligned} \quad (\text{C.2})$$

We thus have

$$U_s |0\rangle = \prod_{j=1}^L \sigma_j^x |0\rangle = \sigma_1^- \sigma_2^- \cdots \sigma_L^- |0\rangle \quad (\text{C.3})$$

Applying the Jordan-Wigner transformation and substituting c_ℓ^\dagger s with \hat{c}_k^\dagger s through (A.10), we have

$$\begin{aligned} \sigma_1^- \sigma_2^- \cdots \sigma_L^- |0\rangle &= c_1^\dagger c_2^\dagger \cdots c_L^\dagger |0\rangle \\ &= \frac{1}{L^{L/2}} \sum_{k_1} \cdots \sum_{k_L} e^{-i(1k_1+2k_2+\cdots+Lk_L)} \hat{c}_{k_1}^\dagger \hat{c}_{k_2}^\dagger \cdots \hat{c}_{k_L}^\dagger |0\rangle \\ &= \frac{1}{L^{L/2}} \left(\sum_{P \in \mathcal{S}_L} e^{(-i \sum_{j=1}^L j k_{P_j})} \epsilon_P \right) \hat{c}_{q_1}^\dagger \hat{c}_{q_2}^\dagger \cdots \hat{c}_{q_L}^\dagger |0\rangle \end{aligned} \quad (\text{C.4})$$

Thus we have the expression (9) of the phase factor A_L . Here we recall that $q_j = (2\pi/L)j$ for $j = 1, 2, \dots, L$ for odd M , and $q_j = (2\pi/L)(j - 1/2)$ for $j = 1, 2, \dots, L$ for even M . We also recall that M denotes the number of down-spins in the sector.

We now calculate the expression (10) for the phase factor A_L . We take a vector $|v\rangle$ with $S_{tot}^z = 0$ as follows. When M is odd, we introduce $\ell = (M - 1)/2$ and we define $|v\rangle$ by

$$|v\rangle = \left(\hat{c}_1^\dagger \hat{c}_2^\dagger \cdots \hat{c}_\ell^\dagger \right) \cdot \left(\hat{c}_{-\ell}^\dagger \cdots \hat{c}_{-2}^\dagger \hat{c}_{-1}^\dagger \right) \cdot \hat{c}_0^\dagger |0\rangle$$

Here \hat{c}_j^\dagger denotes \hat{c}_k^\dagger with $k = (2\pi/L)j$. When M is even, we take $\ell = M/2$, and we define $|v\rangle$ by

$$|v\rangle = \left(\hat{c}_{1/2}^\dagger \hat{c}_{3/2}^\dagger \cdots \hat{c}_{\ell-1/2}^\dagger \right) \cdot \left(\hat{c}_{-(\ell-1/2)}^\dagger \cdots \hat{c}_{-3/2}^\dagger \hat{c}_{-1/2}^\dagger \right) |0\rangle$$

Here $\hat{c}_{j+1/2}^\dagger$ denotes \hat{c}_k^\dagger with $k = (2\pi/L)(j + 1/2)$. Through the operation (7) we can show that $U_s |v\rangle = (-1)^{\ell+1} A_L |v\rangle$ for M odd and $U_s |v\rangle = (-1)^\ell A_L |v\rangle$ for M even. Thus, we have at least $U_s |v\rangle = \pm |v\rangle$.

Let us show that $U_s |v\rangle = +|v\rangle$ for both odd M and even M cases. First we note that $U_s c_1^\dagger c_2^\dagger \cdots c_{L/2}^\dagger |0\rangle = c_{L/2+1}^\dagger c_{L/2+2}^\dagger \cdots c_L^\dagger |0\rangle$. Second, expanding the vector $|v\rangle$ in terms of $c_{j_1}^\dagger c_{j_2}^\dagger \cdots c_{j_{L/2}}^\dagger |0\rangle$ with $1 \leq j_1 < j_2 < \cdots < j_{L/2} \leq L$, we can show that the coefficient of $c_1^\dagger c_2^\dagger \cdots c_{L/2}^\dagger |0\rangle$ in the expansion is equal to that of $c_{L/2+1}^\dagger c_{L/2+2}^\dagger \cdots c_L^\dagger |0\rangle$. Therefore we have $U_s |v\rangle = +|v\rangle$.

Thus, we obtain the expression (10) for the phase factor A_L .

References

- [1] Montambaux G, Poilblanc D, Bellissard J and Sire C 1993 *Phys. Rev. Lett.* **70** 497
- [2] Hsu T C and Anglès d'Auriac J C 1993 *Phys. Rev. B* **47** 14291
- [3] Poilblanc D, Ziman T, Bellissard J, Mila F and Montambaux G 1993 *Europhys. Lett.* **22** 537
- [4] van Ede van der Pals P and Gaspard P 1994 *Phys. Rev. E* **49** 79
- [5] Anglès d'Auriac J C and Maillard J M 2003 *Physica A* **321** 325
- [6] Kudo K and Deguchi T *Phys. Rev. B* 2003 **68** 052510
- [7] Rabson D A, Narozhny B N and Millis A J 2004 *Phys. Rev. B* **69** 054403
- [8] Berkovits R and Avishai Y 1996 *J. Phys. C: Condens. Matter* **8** 389
- [9] Georgeot B and Shepelyansky D L 1998 *Phys. Rev. Lett.* **81** 5129
- [10] Avishai Y, Richert J and Berkovits R 2002 *Phys. Rev. B* **66** 052416
- [11] Santos L F 2004 *J. Phys. A: Math Gen.* **37** 4723
- [12] Kudo K and Deguchi T 2004 *Phys. Rev. B* **69** 132404
- [13] Shklovskii B I, Shapiro B, Sears B R, Lambrianides P and Shore H B 1993 *Phys. Rev. B* **47** 11487
- [14] Nakamura K and Bishop A R 1986 *Phys. Rev. B* **33** 1963
- [15] Nakazono N, Kato T and Nakamura K 2003 *Prog. Theor. Phys. Supp.* **150**, 165
Sawada S *et al.* in preparation.
- [16] Deguchi T, Fabricius K and McCoy B. M 2001 *J. Stat. Phys.* **102** 701
- [17] Fabricius K and McCoy B M 2002 *MathPhys Odyssey 2001* ed M Kashiwara and T Miwa (Boston: Birkhäuser) p 119
- [18] Deguchi T 2002 *J. Phys. A: Math Gen.* **35** 879
- [19] Uglov D B and Ivanov I T 1996 *J. Stat. Phys.* **82** 87
- [20] Meyer H and Anglès d'Auriac J C 1997 *Phys. Rev. E* **55** 6608
- [21] Nagler S E, Buyers W J L, Armstrong R L and Briat B 1983 *Phys. Rev. B* **27** 1784
- [22] Hirata S and Nomura K 2000 *Phys. Rev. B* **61** 9453
- [23] Nomura K and Okamoto K 1994 *J. Phys. A: Math. Gen.* **27** 5773
- [24] Urba L and Rosengren A 2003 *Phys. Rev. B* **67** 104406